JCBI
Journal of Computing & Biomedical Informatics Volume 04 Issue 01
ISSN: 2710 - 1606 2022

Research Article
https://doi.org/10.56979/401/2022/53

Skin Diseases Diagnosis System Based on Machine Learning

Muddasar Abbas[1], Muhammad Imran[1*,] Abdul Majid[2,] and Nadeem Ahmad[1]

[1]Department of Computer Science, BZU, Multan, Pakistan.
[2]Department of Computer Science, Universiti Tun Hussein Onn Malaysia.
[*]Corresponding Author: Muhammad Imran. Email: m.imran@bzu.edu.pk.

Received: January 12, 2022 **Accepted:** October 12, 2022 **Published:** December 29, 2022.

Abstract: Skin diseases are very common across the globe and especially in underdeveloped countries. Increasing climate changes and global warming are among the major causes of cancerous skin diseases. Skin diseases can be deadly if not diagnosed and treated at their initial stages. Clinical skin disease diagnosis methods are very rarely available for a common person and these methods are very expensive as well. The advancement in the field of image processing and machine learning made it possible to use machine learning methods for feature extraction and diagnosis of medical illnesses. Deep learning on the emerging subfields of machine learning methods that are more advance and intelligent in the classification of images based on different features. In this work, different deep learning models are used which are based on Convolution Neural Networks (CNN) architecture like ResNet-50, the DenseNet-121, and sequential CNN model for feature extraction and the classification of skin disease categories using HAM10000 dataset from ISIC archive 2018. The HAM10000 dataset consists of 10015 images from seven different skin disease categories. The dataset is further subdivided into testing and training data with a ratio of 20% and 80% correspondingly. The skin disease diagnosis is a three-step process that includes dataset images preprocessing in the first stage, feature extraction using CNN models in the second stage, and classification of skin disease category based on the extracted features using different classifiers in the third stage. Image augmentation techniques were used to reduce the imbalance in different skin disease classes. The sequential CNN-based model using 7 convolution layers gives an accuracy of 98% and 99% Area Under the Curve (AUC) for all seven skin disease categories. ResNet-50 and DenseNet-121 give an accuracy of 84% and 89% respectively. The performance of different CNN models on the given dataset is compared and evaluated using different performance matrixes.

Keywords: Skin Disease; Machine Learning; Deep Learning; Classification; CNN.

1. Introduction

Skin diseases are among some of the wider spreading diseases among humans. Skin is considered the largest organ in the body of humans that is constantly growing at a very fast rate. Skin acts as a physical barrier between the inner human body and the environment. Human skin is made up of two layers of tissues [1]. The epidermis is the first layer that is also called the outermost layer of skin, it varies in thickness (75-150 μm) and protects the human body from dehydration and other physical and chemical changes in the environment [2]. The second major layer of skin is the dermis which exists underneath the epidermis. The dermis is a connective tissue that is thicker than the epidermis and contains the major mass of human skin. The dermis contains extensive nerve and vascular networks, sweat glands, and keratinized structures which includes sebaceous and hair glands [3].

The epidermis majorly consists of keratinocytes cells that are very important for skin repair, and go through the terminal differentiation process in upward migration for the formation of the outer protective

layer of skin. Epidermis also contains basal cell layers that consist of melanocytes that contain melanin pigment that gives the skin color [4]. The epidermis is further divided conventionally into four components based on keratinocytes each of the components is different from other components based on biochemical and morphological characteristics.

Skin diseases are among the major health issues the world is facing issues nowadays. Various factors can cause skin diseases of numerous types of these factors including excessive exposure to sunlight, different impurities in the blood, fungus, bacteria, viruses, and parasites [5]. Most skin diseases start as abnormal skin growth which sometimes grows into malignant types of skin tissues. Skin diseases are divided into two major groups benign skin diseases and malignant skin diseases. Benign or non-cancerous skin diseases are the most common skin diseases which are not deadly and can be cured effectively [6]. Benign skin diseases mostly include different types of moles which appear on different parts of the skin in early childhood and during the early 20 years of a person's life. Benign skin diseases also include different types of skin growths with vary in color and size e.g., Seborrheic Keratosis [7]. Malignant skin diseases include those skin growths that are very dangerous and can be deadly if not diagnosed in the early stages. Skin cancers are the most frequent type of cancer worldwide [8]. According to a survey by [9], every 5th person in America by the age of 70 years develops skin cancer. Skin cancer type melanoma causes death to more than 5400 people every month worldwide. The treatment of Melanoma and other skin cancers is only possible if detected at the early stage of development [10]. Dermatologists often diagnose skin diseases by observing the infected area of the skin. The diagnosis of skin disease by medical experts is usually based on the generalization capability of the exports which is not reliable every time because of the insufficient amount of available data and the dependency of exports on a standardized method of dermatoscopy that involve microscopic examination of the digital skin disease image [11]. The recent advancement in medical technology based on photonic and lessor technology has made the diagnosis of skin disease faster and more accurate, but because of the high cost of this technology, the use of this technique is very expensive and limited to very few hospitals. Recent development in science and technology enables us to make use of diagnosis based on computer-aided models for the classification of skin diseases based on symptoms of the disease [12]. Image processing plays an important part in the medical science field. Image processing utilizes machine learning (ML) models for the classification of different categories of images in many fields. The role of machine learning is vital in the detection of various types of diseases in the medical science field with the help of different disease datasets[13].

Machine algorithms increase accuracy by training over multiple datasets. These models are trained using three methods of learning, which include supervised, reinforcement, and unsupervised learning [14]. The most basic type of learning is supervised learning in which the model is trained using labeled data. Supervised learning is very useful for small training datasets which are part of a large dataset [15]. Unsupervised learning is the type of machine learning in which the training data is unlabeled. Unsupervised learning is useful to work with large datasets [16]. Reinforcement learning is based on rewarding desired behavior and punishing undesired ones. It uses a trial-and-error method for learning from new situations and improving its accuracy. In most conditions, supervised and unsupervised learning is used [17].

Deep learning (DL) is one of the emerging subfields of machine learning methods that is more advance and intelligent in the classification of images based on different features. DL uses multiple layers to gradually extract high-level features from unprocessed data [18]. The convolutional neural network (CNN) is the most extensively used DL algorithm for the classification of images of different diseases achieving significant performance over the rivaling human exports of the medical science field [19]. Models based on deep learning are more efficient while performing the classification process using images and data. DL algorithms can be used for unsupervised as well as supervised learning tasks.

The demand for the precise identification of abnormality and classification of the right category of the disease by using Magnetic resonance imaging (MRI), X-ray, Computer Topography (CT) images, and the signal data like Electroencephalogram (EEG), the Electrocardiogram (ECG), and Electromyography (EMG) is increasing in the field of medical science [20]. The better treatment of the patient is assisted with the precise identification of the category of the disease. Skin diseases unlike most other diseases require an extensive amount of preciseness for the detection and diagnosis process.

Doctors often diagnose skin problems by checking how they look for detailed diagnoses skin tests are conducted to check the type of skin infection. Doctors use Patch testing to manually diagnose skin allergies.

Patch testing involves applying adhesive patches comprising test substances for a period [21]. The reaction of the skin against the test substance is examined after removing the patch. Skin Bioscopy involves the diagnosis of a benign or a malignant type of skin disease. During bioscopy, the infected portion of the skin is removed and taken to the laboratory for further examination [22]. The infected portion of the skin might be removed using a razor blade or a scalpel tool and stitches are to close the wound. A culture test is used to identify which type of microorganism is causing infection. Culture is performed using a sample of the patient's wound or ulcer. The Sample is collected from the surface of the wound using a swab of sterile cotton [23]. The microorganisms causing skin infections can include viruses, bacteria, and fungi.

The doctors used the ABCD for the Diagnosis of skin cancer at the initial. The ABCDE rule is an important method used for the immediate diagnosis of skin cancer [24]. Doctors can diagnose skin cancer based on the observation of the skin of the patient using this method.

1. A – Asymmetry: One half of the lesion is not like another half
2. B – Borders: Poorly defined or irregular borders of the skin
3. C - Color: The color of skin varies in different areas of skin commonly shades of black, brown, red, or blue
4. D- Diameter: The diameter of the skin lesion is 6mmor larger
5. E – Evaluation: The skin of the cancerous lesion appears dissimilar from the rest changing in shape, size, color

1.1 Using Deep Learning for Skin Disease Classification

Deep leering-based models can help in solving critical problems by identifying input data features automatically and all deep learning algorithms are adaptive to change according to the problem. In this work, an approach based on deep learning that uses CNN (Convolutional Neural Networks) is used for the classification of skin diseases. The proposed model uses a dataset from an online repository of skin disease images called 'International Skin Imaging Collaboration (ISIC)". The dataset is commonly known as HAM10000 which consists of over 10000 images from seven skin diseases, including Dermatofibroma, Benign keratosis-like lesions, Vascular lesions, Melanocytic nevi, Actinic keratoses, Basal cell carcinoma, Melanoma, and Intraepithelial carcinoma [25]. A random function is used for dividing the dataset into training and testing sets. The datasets are unbalanced and contain more images of some diseases and fewer images of some diseases to overcome this issue data augmentation is used. The data augmentation techniques solve the problem of generating more images with the help of rotation or transformation of images from existing images of each skin disease [26]. The CNN-based model is trained on the dataset for classifying different categories of skin disease categories. The model uses a sequential approach with multiple CNN layers. CNN models are used because CNN models do not require extensive image preprocessing and are more accurate in image processing tasks.

The CNN model used takes the image of skin disease as input and associates the corresponding weight with that image for classification and feature extraction. The associated weights are adjusted in such a way that it reduces errors during classification. CNN models have four kinds of layers that include primary convolutional layers, secondary ReLU layers, fully connected layers, and pooling layers. CNN models have a convolutional layer as the model's first layer. The convolutional layer intends to accurately detect the set of features from input images and the formation of feature maps [27]. The pooling layer is usually inserted between two of the convolutional layers. The pooling layer receives maps of multiple features, and it uses pooling operations on those feature maps. The pooling operations consist of reducing the size of input images while retaining their vital characteristics. The pooling layer decreases the number of parameters and calculations required in a network and improves network efficiency by avoiding overlearning [28]. The ReLU describes a nonlinear activation function. The ReLU layer replaces values that are negative in a feature map with zeros. The fully connected layer functions as the last layer of every single neural network that might be convolutional or not, so fundamentally it is not the characteristic layer of CNN [29]. The fully connected layer receives an input vector, and it generates a new output vector. For this purpose, it applies a linear combination and activation function to the input received. Fully connected layers are used in neural networks for classifying the input images [30].

The first block of a CNN model consists of convolutional layers which behave as feature extractors. The first layer uses different several convolutional kernels to filter the image and return the feature map.

These feature maps were then normalized using the activation function. The process of feature extraction can be repeated many times to get more feature maps those feature maps are filtered and finally the final feature maps are concatenated to form a vector [31]. The second block of CNN is also called the end of neural networks used for classification purposes. In this block, the input vectors are transformed using different activation functions. The last vector contains the number of elements equivalent to the number of classes The last layer of this block is used for the calculation of probabilities which uses logistic or SoftMax function depending upon the nature of the input [32].

2. Proposed Methods

Skin diseases are the most common widespread disease found in humans all over the world. The diagnosis of skin disease at the initial stage is very important for their treatment. The laboratory methods for diagnosis of skin diseases include the use of X-Ray, MRI machines, and laboratory analysis of the infected area of the skin. The laboratory tests for skin disease diagnosis require trained professionals. The appearance of skin remains the same in most skin diseases, which makes it very difficult for the dermatologist to correctly diagnose the exact type of skin disease based on the visualization of infected areas and laboratory test results. The dermatologists normally form their diagnosis opinion based on the visualization of the skin, which leads to further analysis of the skin so that their diagnosis opinion can be validated using laboratory analysis of the skin [33]. In underdeveloped countries where dermatologists are not available in small cities and rural areas, the dependency upon exports can be quite a challenging task in case of an urgent medical need. The Laboratory methods required extensive use of electricity which can be challenging in summer when the consumption of electricity increases.

The proposed methodology is divided into the acquisition of data, data preprocessing, splitting images into training and testing datasets, data augmentation, feature extraction, model selection, training the model, and the classification of skin diseases. In figure.1 the architecture of the proposed model is drawn.

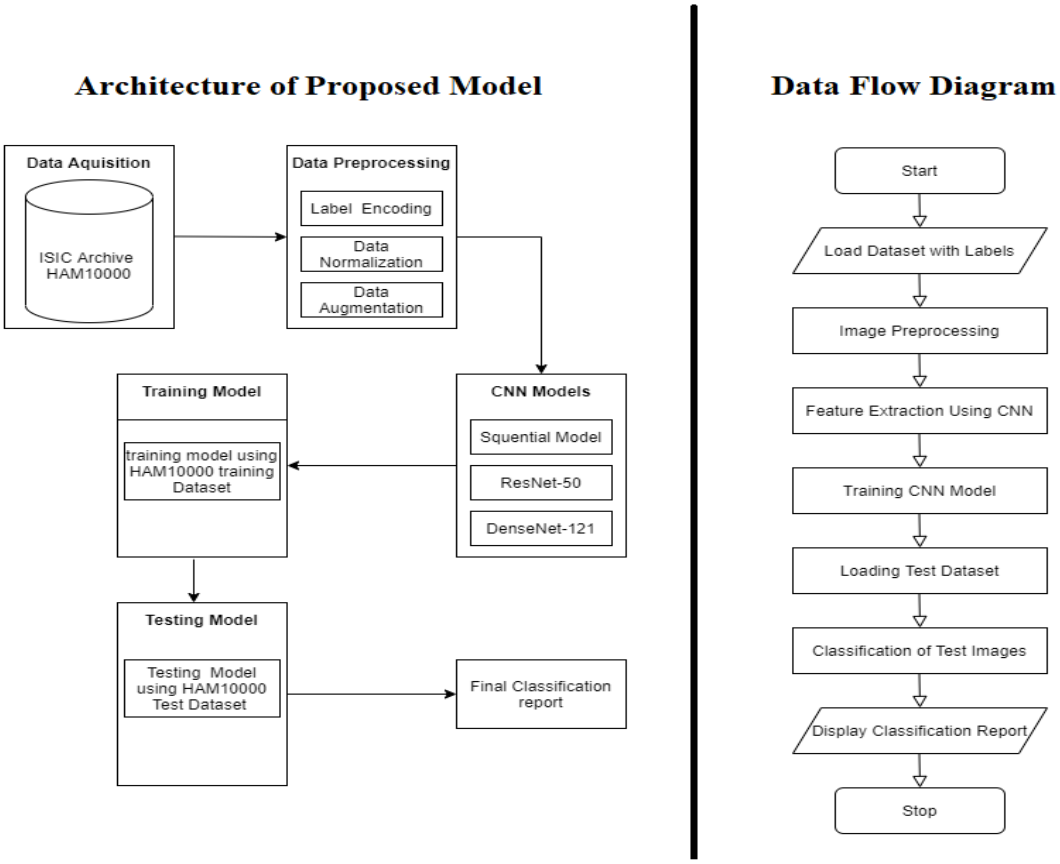

Figure 1. Architecture of the model using ISIC HAM10000 datasets

2.1 Data Collection

The training process of many neural networks for automated detection of skin lesions is largely affected by the small dataset size and lack of diversity in given datasets of skin diseases. The ISIC archive subset HAM10000 dataset containing 10015 images of seven different skin diseases is used. HAM10000 is taken from the ISIC archive which is treated as a collection of multiple datasets of dermoscopy containing 23665 images of different skin lesions. The collection is largely based on melanotic lesions because out of 23665 images 20795 are nevi or melanomas. The HAM10000 is used to enhance the training and testing process of an automated neural network-based model. Table 1 shows the overview of ISIC 2018 dataset classes and their distribution.

Table 1. Overview of ISIC achieve 2018 dataset class distribution

Class	Abbreviation	Class	No. of Images
0	AKEIC	Brown diseases	334
1	BCC	Basal Cell Carcinoma	538
2	BKL	Benign Keratosis-like Lions	1674
3	DF	Dermatofibroma	122
4	MEL	Melanoma	2177
5	NV	Melanocytic Nevi	18618
6	VASC	Vascular Lesions	157
		Total	**23,665**

Table 2 shows different features that the HAM10000 dataset contains about each image in the dataset in the form of a table that contains different features of an image of some skin disease category. These features include image_id, lesion_id, dx, dx_type, sex, age, localization.

Table2. Features of HAM10000 Dataset

Sr.	Features
1	Lesion id (7470 unique values)
2	Image_id (10015 unique values)
3	Dx (seven classes of skin diseases abbreviations e.g., nv, mel, bcc)
4	Dx_type (histo or follow-up)
5	Age
6	Sex (male, female, or others)
7	Localization (localization of skin disease)

At the end of a sequence of layers including convolutional layers, ReLu layers, pooling layers, and nonlinear layers, there is a requirement for a connected layer. The output from the final pooling or convolution layer is flattened and then provided to the fully connected layer as an input. The process of flattening involves the conversion of a 3D matrix into vector values [30].

The output of a fully connected layer is an N-dimensional vector, where N is the number of existing classes from which the model selects a predicted class. The HAM10000 dataset is used for training the model that contains seven classes. Figure 3 shows a sequence of layers that ends with a fully connected layer which gives a 7-dimensional vector containing seven classes from which the neural network selects the desired class for the prediction of skin disease for that input image.

In figure 2 the third portion shows the architecture of the fully connected layer used in the proposed system that helps in the classification of seven types of skin disease which include melanoma, vascular lesions, melanocytic nevi, actinic keratosis, basal cell, and dermatofibroma.

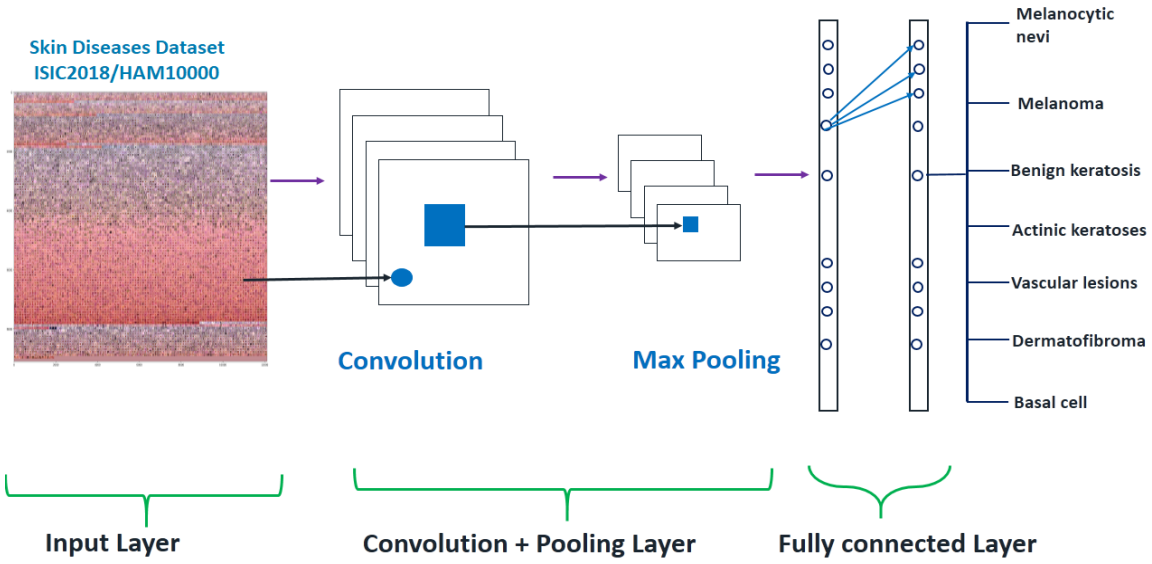

Figure 2. CNN Architecture with a fully connected layer for Skin disease classification

2.2 Building model

In this work, the sequential model is utilized. Sequential is one of the easiest ways to build a model using Keras. This approach allows us to build our model by adding layers sequentially one after another. The function add () is used for adding new layers to the model. Figure 3 shows the model used in this work using the sequential technique.

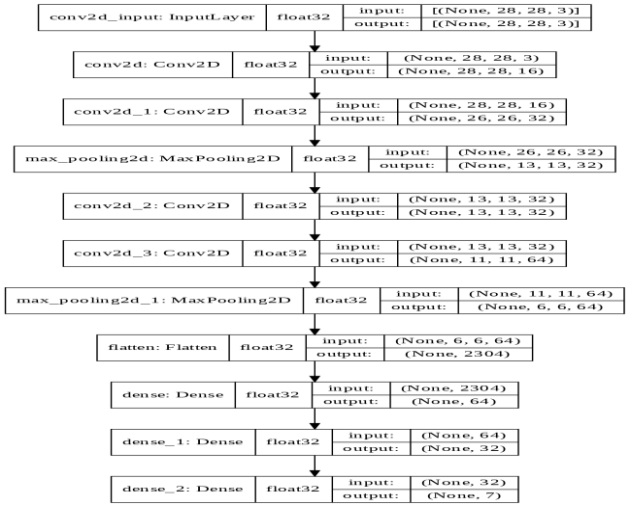

Figure 3. Layering Sequence of Sequential Proposed Model

The model shown in figure 4 requires an image size of 28x28x3. The model starts with two conv2D layers following is a maxpooling2D layer. The model uses conv2D and maxpooling2D layers in different combinations. The first two layers use the ReLu as a function of activation. The dense layer was used as the layer of output and the activation function used in this model is SoftMax. The SoftMax activation function is used because the output of the SoftMax function is a vector range between 0 and 1 which sums up to 1. Compiling the proposed CNN model involve three parameters optimizer, metrics, and loss. The learning rate of the model is controlled using an optimizer. In this work, Adam optimizer is used. The optimizer Adam is used to adjust the rate of learning in the process of training the model. Here learning rate is used to determine the rate at which calculation of model weights takes place. A smaller learning rate gives more

accurate weights but the computation time of the weights increases. The accuracy metric is used to see training accuracy scores. In this work, Categorical Cross entropy is used as a loss function. This is the most used loss function for multiclass classification. The lower score indicates better performance of the model.

Model fitting is used to determine in what way a model generalizes similar data to that of the training data. A well-fitted model gives more accurate results. The fit() function is used to train our model using x_train, y_train, number of epochs, and validation data parameters. The validation is a split of the training dataset used for the model validation purpose. The number of epochs defines how many times the model will go through all the datasets. The increasing number of epochs increases the efficiency to a certain point. After that specific point, the improvement in the model accuracy is stopped. The right number of epochs is very important for training the model more efficiently. In this work, while using a sequential model 40 epochs are used with a batch size of 128. Passing the whole dataset is very difficult which is why the dataset is passed to the model in different sets or batches. The number of iterations defines the number of batches needed for the completion of one epoch. The proposed model uses 234 iterations to complete one epoch while the batch size is 128.

3. Results

In this section of the work, the proposed model's results are discussed and evaluated using different matrixes. The CNN model based on the multiclass classification model is trained over the HAM10000 dataset. The results of the models are evaluated with the help of parameters like validation and training loss, and accuracy of training and validation. These parameters help us determine the CNN model's capabilities. The model performance is evaluated with the help of approaches that involves specificity, accuracy, and sensitivity. The model's performance is evaluated using various evaluation matrixes.

The confusion matrix is a table generally applied to explain the classification model performance, on a given set of data having known true values. The confusion matrix is one of the most common matrices to show the recall and precision of a model. The confusion matrix shows the summary of the estimated outcomes of a classification problem. The confusion matrix is a technique to know what the model is doing in the right direction and where the model is making errors. In table 3 contents of the confusion, matrix is shown.

Table 3. Confusion Matrix of Binary Classification

	PN (Predictive Negative)	**PP (Predictive Positive)**
Actual Positive	False Negatives	True Positives
Actual Negative	True Negatives	False Positives

In table 3 the relation between the actual and predictive classes is shown. Real values are shown in the actual class and the predictive class represents the values predicted with the help of the model. The accuracy of a model depends upon the number of false positive (FP) and false negatives (FN) are lowest as possible and the number of true negatives (TN) and true positives (TF) are highest as possible. These four factors help in analyzing the model. False Positive (FP) denotes the prediction made by the model in which the negative class is incorrectly predicted as the positive class. e.g., if the patient doesn't have melanoma and the model predicts it as a melanoma skin disease, then this prediction can be considered a false positive. False Negative (FN) refers to the predictions made by the model where the positive class is incorrectly predicted as the negative class. e.g., if the patient had melanoma, but the proposed model predicted it as a benign skin disease, then this prediction will be a false negative prediction.

True Positive (TP) mentions the prediction made by the proposed model where a positive class is correctly predicted as a positive class. e.g., if the patient has a melanoma skin disease, and the proposed model is also precited as the melanoma skin disease, then this prediction will be a true positive. True Negative (TN) represents all the correct predictions made by the model where the proposed model correctly predicts a negative class as negative classes e.g. A patient doesn't have the melanoma skin disease and the model also predicted as a patient not having melanoma., then the prediction will be a true negative

The accuracy measures the performance of the machine learning classification model. The classification model's accuracy is determined, by dividing the total number of predictions that are accurate by the total number of predictions of the model. The accuracy gives the best overview of how well a model will perform on a certain dataset. The best accuracy scores are expected when the database is balanced. The balance dataset means every class in the dataset is having nearly an equal number of objects for training the model.

$$\text{accuracy} = \frac{\text{TP} + \text{TN}}{\text{FP} + \text{FN} + \text{TP} + \text{TN}}$$

The model accuracy is additionally divided into testing and training accuracy. The training accuracy is the model accuracy over the dataset for training purposes. The validation or test accuracy is the model accuracy over the test or validation dataset. Figure 4 shows the training and testing or validation accuracy curves for the proposed model using CNN sequential approach.

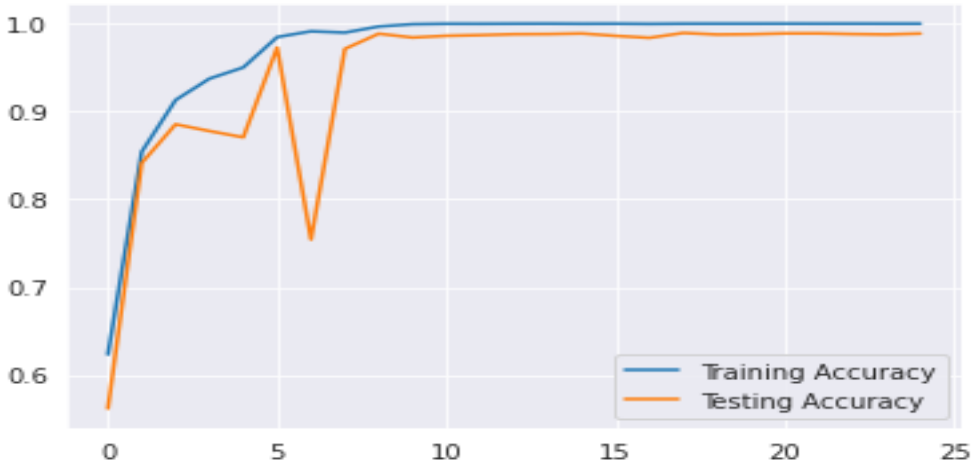

Figure 4. training and testing accuracy curves

The training accuracy shows how well the model is performing over the existing training dataset. The validation or testing accuracy shows how well the model will perform in the case of the new dataset. The first proposed model gives an accuracy of 100% over the training dataset and gives an accuracy of 98% over the validation or testing dataset.

The loss of loss function is another measurement of the performance of the model. The loss function is used for the optimization of the classification model. The loss is calculated on both training and validation or testing datasets. The loss shows how well the model is performing on a given dataset. The loss is the collective sum of all the errors the model is making on training or validation datasets. The loss shows how poorly or how well the model is performing after each iteration.

The specificity can be termed as the rate of true negatives. Specificity shows the number of actual negatives that the model predicts as negatives. This also shows there is some portion of actual negatives that are predicted as positives which are termed as false positives.

$$\text{Specificity} = \frac{\text{TN}}{(\text{TN} + \text{FP})}$$

The Sensitivity represents the measure of the total number of actual positives that the model predicted accurately as positives. The sensitivity of the model can also be termed as the rate of true positives. This also shows there is a portion of actual positives that the model predicted as negatives, termed false negatives.

$$\text{Sensitivity} = \frac{\text{TP}}{(\text{TP} + \text{FN})}$$

The classification report shows the quality of predictions made by a classification model. The classification report is a metric for performance evaluation of a classification model. The classification report is used to show recall, precision, f1-score, and support of the proposed classification model. The classification gives a better overall view of the classification model performance. The classification report shows values

for f1-score, recall, and precision for each class of the classifier model. The SK-learn library in python language is imported for using classification reports. The classification report shows precision, f1-score, and recalls values for the model on given seven classes of diseases of the skin that include melanocytic nevi(NV), vascular lesions (VASC), benign keratosis lesions (BKL), actinic keratoses (AKIEC), dermatofibroma (DF), basal cell carcinoma (BCC), and melanoma (MEL). The classification report also includes micro, macro, weighted, and sample averages. The proposed model's classification report is shown in Figure 5.

	precision	recall	f1-score	support
('akiec', 'Actinic keratoses and intraepithelial carcinomae')	1.00	1.00	1.00	1667
('bcc', ' basal cell carcinoma')	0.99	1.00	1.00	1689
('bkl', 'benign keratosis-like lesions')	0.97	1.00	0.98	1651
('df', 'dermatofibroma')	1.00	1.00	1.00	1629
('nv', ' melanocytic nevi')	1.00	0.94	0.97	1663
('vasc', ' pyogenic granulomas and hemorrhage')	1.00	1.00	1.00	1680
('mel', 'melanoma')	0.97	0.99	0.98	1755
micro avg	0.99	0.99	0.99	11734
macro avg	0.99	0.99	0.99	11734
weighted avg	0.99	0.99	0.99	11734
samples avg	0.99	0.99	0.99	11734

Figure 5. Proposed CNN classification model Classification Report

The classification model's precision is its capability to correctly recognize only relevant data points. Precision shows the percentage of the relevant results. The model person is a ratio among the summation of total true positives and false positives with the total true positive numbers. Precision shows how accurate are the predictions of the model. In figure 4.4, the precision of the proposed model using the sequential CNN approach is given. The precision for four categories of skin disease actinic keratosis (AKIEC), dermatofibroma (DF), basal cell carcinoma (BCC), and vascular lesions (VASC) is exactly one means the proposed model predicts these four skin disease categories with 100% accuracy. The precision score of the proposed model is 0.95 for melanoma (ML), 0.97 for benign keratosis (BKL), and 0.99 for melanocytic nevi (NV).

The Roc curve is used to plot TPR and FPR at different intervals during the classification process of a model. The ROC curve analysis offers the means to pick possibly ideal classification models and to dispose of deficient ones autonomously from the distribution of the class. The ROC curve analysis is a straightforward and accurate mean of benefit/cost analysis in analytical decision-making. The ROC curve progress shows the relationship between specificity and sensitivity. As a starting point, any random classifier is used to give points residing alongside the x-axis (FPR = TPR). The bending of the ROC curve towards a 45-degree angle from the diagonal shows the decreasing accuracy of the model. In figure 6 the ROC curve is shown for the proposed Model on the ISIC 2018/HAM10000 dataset.

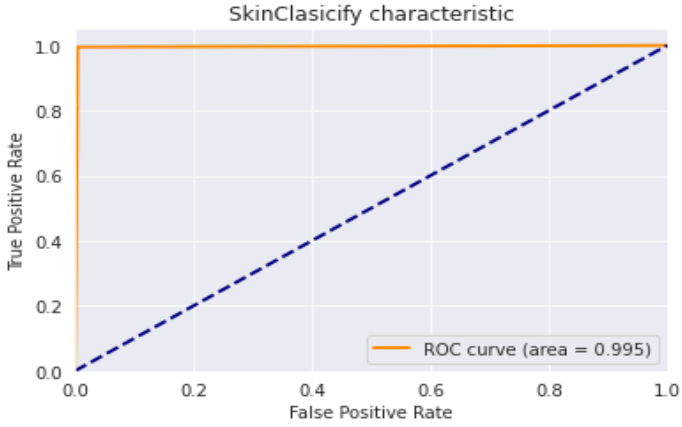

Figure 6. ROC of the Sequential CNN model

The ROC curve of convolutional neural networks proposed in this work based on a sequential approach is shown where the value AUC of the ROC curve is 0.995. AUC is the two-dimensional area of the ROC curve. The value of AUC varies from 0 to 1 where the best performing model has an AUC value closer to 1 and poor models have values under 0.5. Figure 7 shows ROC curves for seven classes of the HAM10000 dataset.

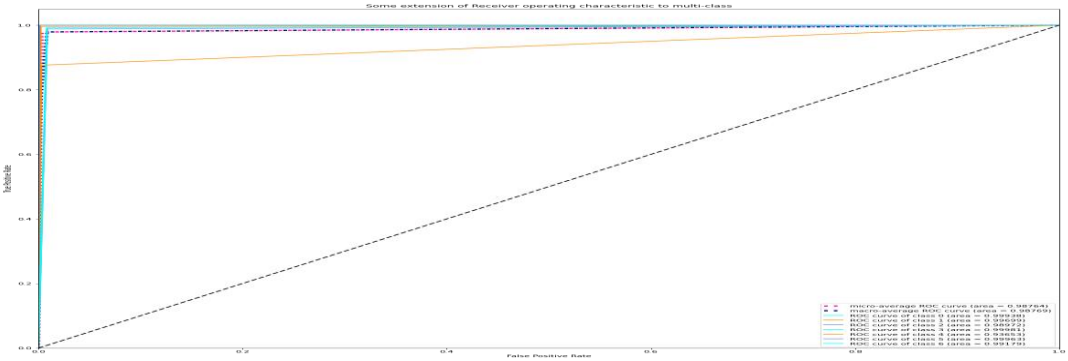

Figure 7. ROC curves for HAM10000 seven classes

In figure 8 the ROC curves are shown for all seven skin disease categories present in the HAM10000 dataset. The AUC values for all skin disease categories are shown in the figure. Class 0 represents Actinic keratosis (AKIEC) which has AUC=0.99938. Class 1 represents basal cell carcinoma (BCC) and has AUC=0.99699. Class 2 represents benign keratosis (BKL) and has AUC=0.98972. Class 3 representing dermatofibroma (DF) has AUC=0. 99981. Class 4 representing melanocytic nevi has AUC=0.93653. Class 5 representing Vascular lesions (VASC) has AUC=0.99963. Class 6 representing melanoma has AUC=0.99179. The AUC values for all seven skin disease categories are above 0.99 which implies the performance of the model is very much accurate in the diagnosis of every skin disease category.

3.1 Model Performance

The accuracy of the model based on Resnet-50 is 0.90187 on the training dataset and 0.8438 on the validation dataset. The HAM10000 dataset is distributed into validation and training datasets with a ratio of 20% and 80% respectively. The accuracy of the model varies in the diagnosis of different skin diseases where the number of samples available for training and the testing purpose is not equal. Figure 8 shows the graph of validation and training accuracy together with testing and training loss of the Resnet-50 model.

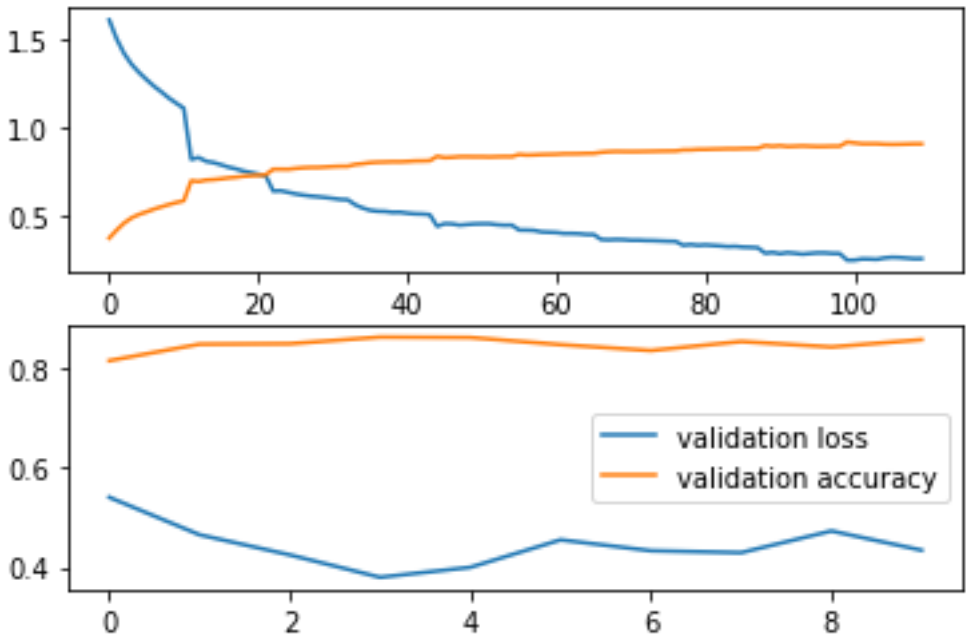

Figure 8. training and validation loss and accuracy of Resnet50-based model

The confusion matrix and classification report of the Resnet-50-based model is given below which shows the details of the performance of the model on 10 epochs. Figure 9 shows the Confusion matrix of the Resnet-50-based model.

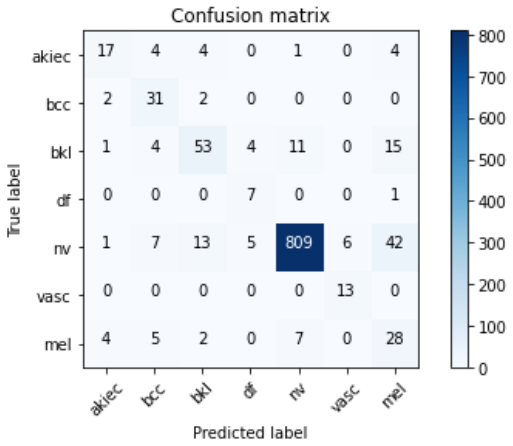

Figure 9. Confusion matrix of resnet50 model

Figure 10 shows the classification report of the Resnet-50-based model. The classification report of the model shows the values of precision and recall vary in between different categories of skin disease. The value of precision is very low for melanoma (ML) and dermatofibroma (DF) because the numbers of training and validation samples for these categories are very low as compared to other skin disease categories like melanocytic nevi (NV). The model's accuracy increases with the help of increasing the training samples of datasets.

	precision	recall	f1-score	support
akiec	0.68	0.57	0.62	30
bcc	0.61	0.89	0.72	35
bkl	0.72	0.60	0.65	88
df	0.44	0.88	0.58	8
nv	0.98	0.92	0.95	883
vasc	0.68	1.00	0.81	13
mel	0.31	0.61	0.41	46
accuracy			0.87	1103
macro avg	0.63	0.78	0.68	1103
weighted avg	0.90	0.87	0.88	1103

Figure 10. Resnet-50 classification report

The accuracy of the DenseNet121-based model is 0.93028 on the training dataset and 0.89274 on the testing dataset. The training and the testing dataset ratio are 80 % and 20 % respectively. The values of accuracy on the validation dataset vary among different skin disease categories where the numbers of training samples are not equal. Figure 11 loss and accuracy curves are shown for testing and training datasets.

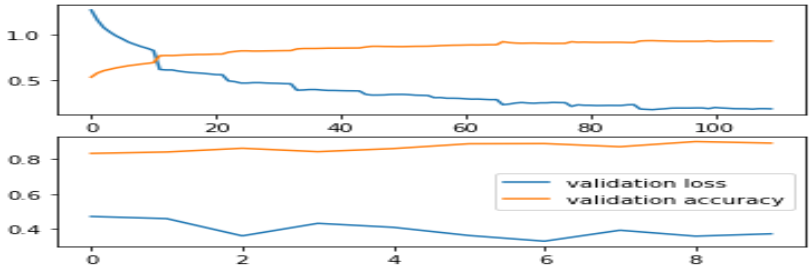

Figure 11. Densenet121 training and testing accuracy and loss

Figure 12 shows the confusion matrix of the Densnet121-based model

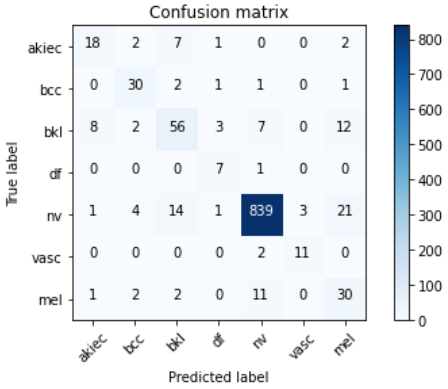

Figure12. Densenet121 confusion matrix

Figure 13 shows the classification report of the DenseNet121 based model.

	precision	recall	f1-score	support
akiec	0.64	0.60	0.62	30
bcc	0.75	0.86	0.80	35
bkl	0.69	0.64	0.66	88
df	0.54	0.88	0.67	8
nv	0.97	0.95	0.96	883
vasc	0.79	0.85	0.81	13
mel	0.45	0.65	0.54	46
accuracy			0.90	1103
macro avg	0.69	0.77	0.72	1103
weighted avg	0.91	0.90	0.90	1103

Figure 33. DesneNet121 classification report

The classification report shows variations in precision and recall values for each skin disease category of the HAM10000 dataset. Most of the skin disease classes have precision values greater than 60%, and melanoma (ML) and dermatofibroma (DF) are the categories having precision and recall values lesser than other categories. Precision and recall vary between skin disease categories because the dataset has a different number of samples for each category.

The accuracy of the CNN model was 0.9686 on the training dataset and 0.9561 on the test or validation dataset. After improving by adding 7 convolutional layers instead of 4 and applying batch normalization, the accuracy of the CNN model on the training dataset is 1.0 and 0.9878 on the test or the validation dataset. Figure 14 shows the accuracy on training and testing sets for the proposed model before and after improvement in layers.

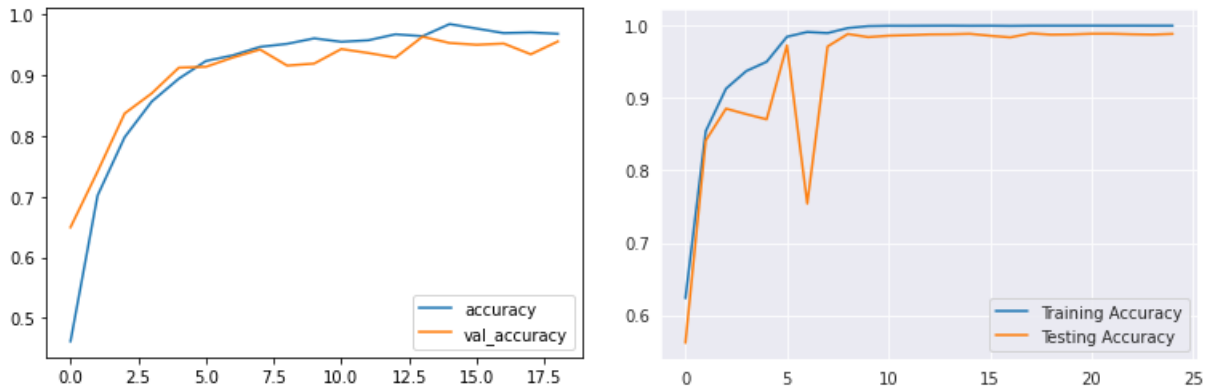

Figure 1 Error! No text of specified style in document.. accuracy of CNN Model before and after changing layers

The left portion of figure 14 presents the model training and validation accuracy before improving the layered structure of the model and the figure is presenting the training and validation accuracy after implementing the improved layered structure with batch normalization on the right side. Figure 15 demonstrates the classification reports of the CNN model before and after improvement in the layer structure.

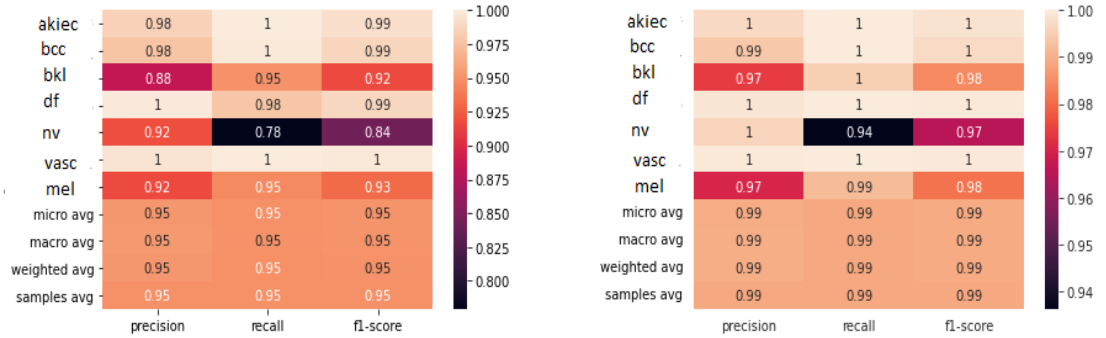

Figure 15. Classification report of Proposed CNN Model

The classification report shows improvement in precision and recall of the skin disease categories having a smaller number of training samples. The precision and recall values of every category of skin disease show substantial improvement. Figure 16 shows the confusion matrix of the CNN model before and after changing the layers and applying batch normalization.

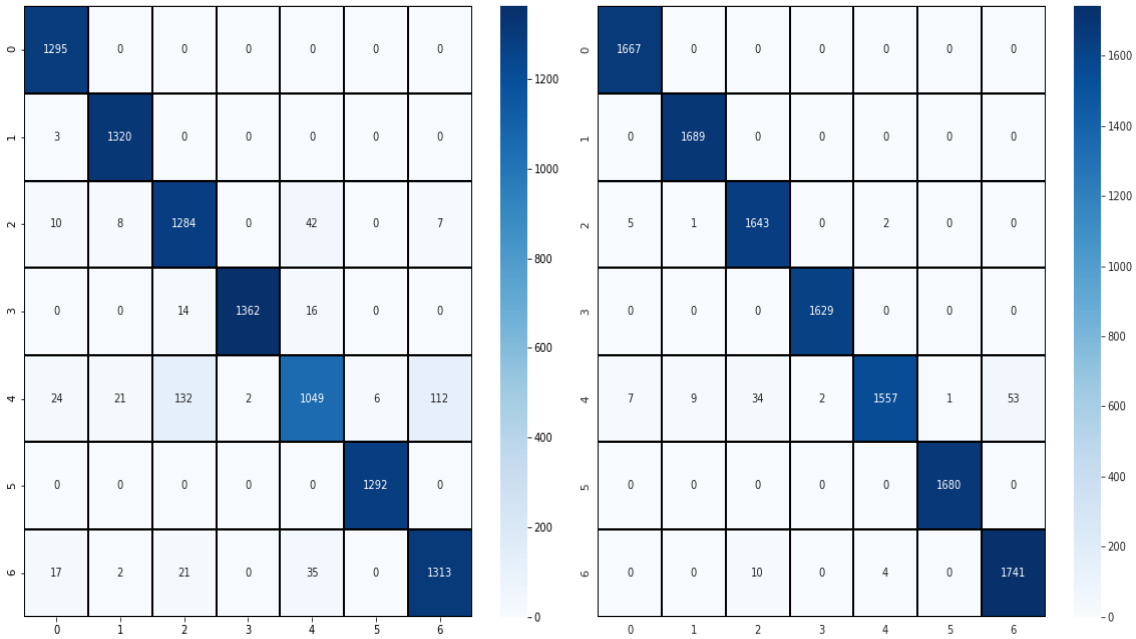

Figure 16. Confusion matrix of Proposed CNN Model

In figure 16 left side is showing the confusion matrix before optimizing the layers and the right side is showing the confusion matrix after applying the layer optimization, substantial improvement can be seen in the prediction accuracy of the model. The total of true positives increases and the total of false positives decreases in almost every class of skin disease. The CNN model before optimization was predicting about 1300 samples accurately, but after applying the optimization the model can accurately predict about 1600-1700 samples of each class of skin disease available in the HAM10000 dataset.

3.2 Comparison of different CNN Models on the HAM10000 dataset

In this work, three different CNN models are used including ResNet-50, DenseNet-121, and sequential CNN model. In table 4 the comparison of CNN models is shown in terms of accuracy, precision, and recall. All the models give above 80% accuracy on the HAM10000 dataset.

Table Error! No text of specified style in document.. Comparison of different CNN models

Model	Accuracy	Precision	Recall	Avg F1-score
ResNet-50	84%	63%	78%	68%
DenseNet121	89%	69%	77%	72%
Sequential CNN	98%	99%	99%	99%

The comparison of CNN models is shown in table 4 where the accuracy of the proposed CNN model using a sequential approach is much higher than the other two models used the layer optimization further increased the model accuracy. The validation or testing accuracy of the ResNet50-based model is 84%, and the DenseNet121 model training accuracy is 89%. The CNN sequential model has a validation accuracy of 98%. The precision and recall values for the sequential CNN model are 99% which is much higher than the other two models.

4. Discussion & Conclusions

Skin diseases are among some of the most common diseases in the world. Nowadays due to climate change and global warming, the number of cancerous and deadly skin diseases is increasing day by day. In underdeveloped countries like Pakistan, the early detection of skin diseases is very difficult. Most skin diseases are curable if diagnosed and treated at the early stages. This study is based on the diagnosis of skin diseases using different deep learning-based models like ResNet-50, DenseNet-121, and the Sequential CNN model. The major focus of our study is to build and train the model based on Convolutional Neural Networks (CNN) sequential approach having 7 convolution layers with effective batch normalization on the ISIC archive HAM10000 dataset. The HAM10000 consists of 10015 images from seven skin disease categories. The given dataset is subdivided into training and testing sets having a ratio of 80% and 20 % respectively. The dataset is augmented to reduce class imbalance and prevent the model from overfitting. The accuracy of the ResNet-50 model is 91% on the training dataset and 84% on the testing or validation dataset. The accuracy of DenseNet-121 is 93% on the training dataset and 89% on the validation dataset. The model proposed based on CNN sequential approach with 7 convolutional layers has a training accuracy of 100% and validation or testing accuracy of 98% on the HAM10000 dataset. The ROC curve of the proposed model has an AUC value above 99% for every category of skin disease in the dataset. The prediction accuracy of the model was better for skin disease categories where the number of samples was more than in other categories. The work included different performance matrixes for evaluating the performance of the proposed model. The comparison of different CNN models is done in terms of recall, precision, f1-score, and accuracy for confirmation of results of testing and training. The proposed deep learning approach is not intending to replace current disease-diagnostic solutions. The study aims to supplement existing skin disease diagnosis solutions. Clinical laboratory tests are always more effective than the prediction of skin diseases based on just the visualization of the skin.

The proposed CNN model needs a more substantial number of parameters for improved accuracy. The fetched input image and the CNN model's resulting output have no significant chance to discover all possible patterns in the image during the assessment process. The CNN model can be used with image processing techniques like GLCM to further enhance the process of feature extraction. The model can be additionally improved by integrating the self-learning ability and knowledge gathering from its early experiences. The efforts on training the model can be considerably reduced by using high-quality images with an enhanced set of features. It is recommended for future research be performed to investigate the feature extraction procedures utilizing biomarkers, even though there is sufficient data, depending on the specific findings. Biomarkers successfully diagnose skin disease by using supplementary data involving protein sequences, genomic, and pathological data alongside imaging data.

In the future, the skin disease diagnosis systems could include a framework where the model detects the skin disease type and dermatologists cross-verify the report generated by the model. The dermatologist can use their knowledge of the field to increase the prediction accuracy of the model and recommend some treatments regarding skin disease.

References

1. H. Bonifant and S. Holloway, "A review of the effects of ageing on skin integrity and wound healing," Br. J. Community Nurs., vol. 24, no. March, pp. S28–S33, 2019, doi: 10.12968/bjcn.2019.24.Sup3.S28.
2. A. A. Tandara and T. A. Mustoe, "The role of the epidermis in the control of scarring: evidence for mechanism of action for silicone gel," J. Plast. Reconstr. Aesthetic Surg., vol. 61, no. 10, pp. 1219–1225, 2008, doi: 10.1016/j.bjps.2008.03.022.
3. A. Dehdashtian, T. P. Stringer, A. J. Warren, E. W. Mu, B. Amirlak, and L. Shahabi, "Anatomy and physiology of the skin," Melanoma A Mod. Multidiscip. Approach, pp. 15–26, 2018, doi: 10.1007/978-3-319-78310-9_2.
4. M. Murakami, T. Akagi, Y. Sasano, and M. Akashi, "Effect of 3D-Fibroblast Dermis Constructed by Layer-by-Layer Cell Coating Technique on Tight Junction Formation and Function in Full-Thickness Skin Equivalent," ACS Biomater. Sci. Eng., vol. 7, no. 8, pp. 3835–3844, 2021, doi: 10.1021/acsbiomaterials.1c00375.
5. J. Norton, "SECTION II Emergency Imaging , Endoscopy , Laboratory Diagnostics , and Monitoring Laboratory Diagnosis of Bacterial , Fungal , Viral , and Parasitic Pathogens," Equine Emergencies, no. January, pp. 30–32, 2020, [Online]. Available: http://dx.doi.org/10.1016/B978-1-4557-0892-5.00009-X.
6. M. A. Linares, A. Zakaria, and P. Nizran, "Skin Cancer," Prim. Care - Clin. Off. Pract., vol. 42, no. 4, pp. 645–659, 2015, doi: 10.1016/j.pop.2015.07.006.
7. A. Plunkett, K. Merlin, D. Gill, Y. Zuo, D. Jolley, and R. Marks, "The frequency of common nonmalignant skin conditions in adults in central Victoria, Australia," Int. J. Dermatol., vol. 38, no. 12, pp. 901–908, 1999, doi: 10.1046/j.1365-4362.1999.00856.x.
8. D. L. Narayanan, R. N. Saladi, and J. L. Fox, "Ultraviolet radiation and skin cancer," Int. J. Dermatol., vol. 49, no. 9, pp. 978–986, 2010, doi: 10.1111/j.1365-4632.2010.04474.x.
9. American Cancer Society, "American Cancer Society. Cancer Facts & Figures 2021. Atlanta: American Cancer Society; 2021." pp. 1–72, 2021.
10. P. Fontanillas et al., "Disease risk scores for skin cancers," Nat. Commun., vol. 12, no. 1, pp. 1–13, 2021, doi: 10.1038/s41467-020-20246-5.
11. J. D. Johansen et al., "European Society of Contact Dermatitis guideline for diagnostic patch testing - Recommendations on best practice," Contact Dermatitis, vol. 73, no. 4, pp. 195–221, 2015, doi: 10.1111/cod.12432.
12. H. Lee and Y. P. P. Chen, "Image based computer aided diagnosis system for cancer detection," Expert Syst. Appl., vol. 42, no. 12, pp. 5356–5365, 2015, doi: 10.1016/j.eswa.2015.02.005.
13. G. Battineni, G. G. Sagaro, N. Chinatalapudi, and F. Amenta, "Applications of machine learning predictive models in the chronic disease diagnosis," J. Pers. Med., vol. 10, no. 2, 2020, doi: 10.3390/jpm10020021.
14. M. Batta, "Machine Learning Algorithms - A Review ," Int. J. Sci. Res. (IJ, vol. 9, no. 1, pp. 381-undefined, 2020, doi: 10.21275/ART20203995.
15. H. Nisar, Y. K. Ch'ng, and Y. K. Ho, "Automatic Segmentation and Classification of Eczema Skin Lesions Using Supervised Learning," 2020 IEEE Conf. Open Syst. ICOS 2020, pp. 25–30, 2020, doi: 10.1109/ICOS50156.2020.9293657.
16. B. Bozorgtabar, S. Sedai, P. Kanti Roy, and R. Garnavi, "Skin lesion segmentation using deep convolution networks guided by local unsupervised learning," IBM J. Res. Dev., vol. 61, no. 4, pp. 1–8, 2017, doi: 10.1147/JRD.2017.2708283.
17. K.-F. Tang, H.-C. Kao, and C.-N. Chou, "Inquire and Diagnose : Neural Symptom Checking Ensemble using Deep Reinforcement Learning," Nips, no. Nips, pp. 1–9, 2016.
18. P. Ongsulee, "Artificial intelligence, machine learning and deep learning," Int. Conf. ICT Knowl. Eng., pp. 1–6, 2018, doi: 10.1109/ICTKE.2017.8259629.
19. D. Jha, M. A. Riegler, D. Johansen, P. Halvorsen, and H. D. Johansen, "DoubleU-Net: A deep convolutional neural network for medical image segmentation," Proc. - IEEE Symp. Comput. Med. Syst., vol. 2020-July, pp. 558–564, 2020, doi: 10.1109/CBMS49503.2020.00111.
20. M. Siragusa et al., "Skin pathology findings in a cohort of 1500 adult and elderly subjects," Int. J. Dermatol., vol. 38, no. 5, pp. 361–366, 1999, doi: 10.1046/j.1365-4362.1999.00720.x.
21. W. D. James, L. E. Rosenthal, R. R. Brancaccio, and J. G. Marks, "American Academy of Dermatology patch testing survey: Use and effectiveness of this procedure," J. Am. Acad. Dermatol., vol. 26, no. 6, pp. 991–994, 1992, doi: 10.1016/0190-9622(92)70145-6.
22. P. C. Alguire and B. M. Mathes, "Skin biopsy techniques for the internist," J. Gen. Intern. Med., vol. 13, no. 1, pp. 46–54, 1998, doi: 10.1046/j.1525-1497.1998.00009.x.
23. Verghese, "基因的改变 NIH Public Access," Bone, vol. 23, no. 1, pp. 1–7, 2011, doi: 10.1038/jid.2013.387.Organotypic.
24. R. S. Prasad, G. Kumar Singh, S. Prasad, and V. Prasad, "Unique Color Circle Design for A Novel Screening Tool to Identify Cancerous Skin Lesions," Proc. CONECCT 2020 - 6th IEEE Int. Conf. Electron. Comput. Commun. Technol., 2020, doi: 10.1109/CONECCT50063.2020.9198345.
25. P. Tschandl, C. Rosendahl, and H. Kittler, "Data descriptor: The HAM10000 dataset, a large collection of multi-source dermatoscopic images of common pigmented skin lesions," Sci. Data, vol. 5, pp. 1–9, 2018, doi: 10.1038/sdata.2018.161.
26. A. Mikołajczyk and M. Grochowski, "Data augmentation for improving deep learning in image classification problem," 2018 Int. Interdiscip. PhD Work. IIPhDW 2018, pp. 117–122, 2018, doi: 10.1109/IIPHDW.2018.8388338.

27. K. Zhang, W. Zuo, Y. Chen, D. Meng, and L. Zhang, "Beyond a Gaussian denoiser: Residual learning of deep CNN for image denoising," IEEE Trans. Image Process., vol. 26, no. 7, pp. 3142–3155, 2017, doi: 10.1109/TIP.2017.2662206.
28. S. Albawi, T. A. Mohammed, and S. Al-Zawi, "Understanding of a convolutional neural network," Proc. 2017 Int. Conf. Eng. Technol. ICET 2017, vol. 2018-January, pp. 1–6, 2018, doi: 10.1109/ICEngTechnol.2017.8308186.
29. H. Ide and T. Kurita, "Improvement of learning for CNN with ReLU activation by sparse regularization," Proc. Int. Jt. Conf. Neural Networks, vol. 2017-May, pp. 2684–2691, 2017, doi: 10.1109/IJCNN.2017.7966185.
30. A. G. Schwing and R. Urtasun, "Fully Connected Deep Structured Networks," pp. 1–10, 2015, [Online]. Available: http://arxiv.org/abs/1503.02351.
31. K. Pai and A. Giridharan, "Convolutional Neural Networks for classifying skin lesions," IEEE Reg. 10 Annu. Int. Conf. Proceedings/TENCON, vol. 2019-October, pp. 1794–1796, 2019, doi: 10.1109/TENCON.2019.8929461.
32. B. Bayar and M. C. Stamm, "Constrained Convolutional Neural Networks: A New Approach Towards General Purpose Image Manipulation Detection," IEEE Trans. Inf. Forensics Secur., vol. 13, no. 11, pp. 2691–2706, 2018, doi: 10.1109/TIFS.2018.2825953.
33. E. N. Wilmer, C. J. Gustafson, S. A. Davis, S. R. Feldman, and W. W. Huang, "Most common dermatologic conditions encountered by dermatologists and nondermatologists," Cutis, vol. 94, no. 6, pp. 285–292, 2014.
34. K. Korotkov and R. Garcia, "Computerized analysis of pigmented skin lesions: A review," Artif. Intell. Med., vol. 56, no. 2, pp. 69–90, 2012, doi: 10.1016/j.artmed.2012.08.002.
35. N. S. Alkolifi Alenezi, "A Method of Skin Disease Detection Using Image Processing and Machine Learning," Procedia Comput. Sci., vol. 163, pp. 85–92, 2019, DOI: 10.1016/j.procs.2019.12.090.
36. S. Kalaiarasi, H. Kumar, and S. Patra, "Dermatological Disease Detection using Image Processing and Neural Networks," vol. 6, pp. 109–118, 2018.
37. S. Malliga, G. Sherly Infanta, S. Sindoora, and S. Yogarasi, "Skin disease detection and classification using deep learning algorithms," Int. J. Adv. Sci. Technol., vol. 29, no. 3 Special Issue, pp. 255–260, 2020.
38. A. K. Verma, S. Pal, and S. Kumar, "Classification of Skin Disease using Ensemble Data Mining Techniques," vol. 20, no. 2010, pp. 1887–1894, 2019, DOI: 10.31557/APJCP.2019.20.6.1887.
39. T. A. Rimi, "Derm-NN : Skin Diseases Detection Using Convolutional Neural Network," no. Iciccs, pp. 1205–1209, 2020.
40. J. Velasco et al., "A Smartphone-Based Skin Disease Classification Using MobileNet CNN International Journal of Advanced Trends in Computer Science and Engineering Available Online at http://www.warse.org/IJATCSE/static/pdf/file/ijatcse116852019.pdf A Smartphone-Based Skin D," Int. J. Adv. Trends Comput. Sci. Eng., vol. 8, no. October, pp. 2–8, 2019.
41. S. Akyeramfo-sam and D. Yeboah, "A Web-Based Skin Disease Diagnosis Using Convolutional Neural Networks," no. November 2019, DOI: 10.5815/ijitcs.2019.11.06.
42. T. Shanthi, R. S. Sabeenian, and R. Anand, "Microprocessors and Microsystems Automatic diagnosis of skin diseases using convolution neural network," Micro process. Microsyst., vol. 76, p. 103074, 2020, DOI: 10.1016/j.micpro.2020.103074.
43. P. N. Srinivasu, J. G. Sivasai, M. F. Ijaz, A. K. Bhoi, W. Kim, and J. J. Kang, "Networks with MobileNet V2 and LSTM," pp. 1–27, 2021.
44. M. N. Bajwa et al., "applied sciences Computer-Aided Diagnosis of Skin Diseases using Deep Neural Networks," no. Dl, pp. 1–13, 2020, DOI: 10.3390/app10072488.
45. J. Rathod, V. Waghmode, and A. Sodha, "Diagnosis of skin diseases using Convolutional Neural Networks," no. Iceca, pp. 2018–2021, 2018.
46. D. B. Mendes, "Skin Lesions Classification Using Convolutional Neural Networks in Clinical Images," 2017.
47. X. Zhang, S. Wang, J. Liu, and C. Tao, "Towards improving diagnosis of skin diseases by combining deep neural network and human knowledge," vol. 18, no. Suppl 2, 2018.
48. A. Sallam, "Mobile-based Intelligent Skin Diseases Diagnosis System," 2019 First Int. Conf. Intell. Comput. Eng., pp. 1–6, 2019.
49. M. B. Science, "Detection of Cancerous and Non-cancerous Skin by using GLCM Matrix and Detection of Cancerous and Non-cancerous Skin by using GLCM Matrix and Neural Network Classifier," no. December, 2015, DOI: 10.5120/ijca2015907513.
50. V. B. Kumar, "Dermatological Disease Detection Using Image Processing and Machine Learning," pp. 88–93, 2016.
51. S. Samavi, N. Karimi, S. M. R. Soroushmehr, M. H. Jafari, K. Ward, and K. Najarian, "Melanoma Detection by Analysis of Clinical Images Using Convolutional Neural Network," pp. 1–4.
52. S. Sourav, "Automated Detection of Dermatological Disorders through Image-Processing and Machine Learning," 2017 Int. Conf. Intell. Sustain. Syst., no. Iciss, pp. 1047–1051, 2017.
53. N. Deivanayagampillai and K. Jc, "Melanoma Detection in Dermoscopic Images using Global and Local Feature Melanoma Detection in Dermoscopic Images using Global and Local Feature Extraction," no. May 2017, DOI: 10.14257/ijmue.2017.12.5.02.
54. A. I. Paradigms, "Detection of melanoma skin disease by extracting high-level features for skin lesions Vikash Yadav * and Vandana Dixit Kaushik," vol. 11, pp. 397–408, 2018.
55. E. Akar, O. Marques, W. A. Andrews, and B. Furht, Cloud-Based Skin Lesion Diagnosis System Using Convolutional Neural Networks. Springer International Publishing, 2019.
56. A. Murugan, S. A. H. Nair, and K. P. S. Kumar, "Detection of Skin Cancer Using SVM, Random Forest and kNN Classifiers," 2019.

57. K. Polat and K. O. Koc, "Detection of Skin Diseases from Dermoscopy Image Using the combination of Convolutional Neural Network and One-versus-All," pp. 80–97, 2020, DOI: 10.33969/AIS.2020.21006.
58. M. T. C. T. A. Scholar, "images using Transfer Learning Technique," pp. 888–895, 2020.
59. Z. H. E. Wu et al., "Studies on Different CNN Algorithms for Face Skin Disease Classification Based on Clinical Images," vol. 7, pp. 66505–66511, 2019, DOI: 10.1109/ACCESS.2019.2918221.
60. H. M. U. Enes Ayyan, "Data augmentation importance for classification of skin lesions via deep learning," 2018 Electr. Electron. Comput. Sci. Biomed. Eng. Meet., p. 4, 2018.
61. C. Scientists, a T. Harvard, C. Scientists, a T. Mit, T. Up, and T. O. Settle, "What makes a data visualization memorable ?," IEEE Trans. Vis. Comput. Graph., vol. 19, no. 12, pp. 1–6, 2013.
62. K. M. Franklin and J. C. Roberts, "Pie chart sonification," Proc. Int. Conf. Inf. Vis., vol. 2003-January, pp. 4–9, 2003, doi: 10.1109/IV.2003.1217949.
63. K. M. Franklin and J. C. Roberts, "Pie chart sonification," Proc. Int. Conf. Inf. Vis., vol. 2003-January, pp. 4–9, 2003, doi: 10.1109/IV.2003.1217949.
64. S. B. Kotsiantis and D. Kanellopoulos, "Data preprocessing for supervised leaning," Int. J. …, vol. 1, no. 2, pp. 1–7, 2006, doi: 10.1080/02331931003692557.
65. S. B. Kotsiantis and D. Kanellopoulos, "Data preprocessing for supervised leaning," Int. J. …, vol. 1, no. 2, pp. 1–7, 2006, doi: 10.1080/02331931003692557.
66. Y. Li, H. Hu, and G. Zhou, "Using Data Augmentation in Continuous Authentication on Smartphones," IEEE Internet Things J., vol. 6, no. 1, pp. 628–640, 2019, doi: 10.1109/JIOT.2018.2851185.
67. R. Takahashi, T. Matsubara, and K. Uehara, "RICAP: Random Image Cropping and Patching Data Augmentation for Deep CNNs," Proc. Mach. Learn. Res., no. 2012, pp. 786–798, 2018, [Online]. Available: https://github.com/facebook/fb.resnet.torch.
68. Z. Zhong, L. Zheng, G. Kang, S. Li, and Y. Yang, "Random erasing data augmentation," AAAI 2020 - 34th AAAI Conf. Artif. Intell., pp. 13001–13008, 2020, doi: 10.1609/aaai.v34i07.7000.
69. K. Wang, B. Fang, J. Qian, S. Yang, X. Zhou, and J. Zhou, "Perspective Transformation Data Augmentation for Object Detection," IEEE Access, vol. 8, pp. 4935–4943, 2020, doi: 10.1109/ACCESS.2019.2962572.
70. Y. Xi, J. Zheng, X. Li, X. Xu, J. Ren, and G. Xie, "SR-POD: Sample rotation based on principal-axis orientation distribution for data augmentation in deep object detection," Cogn. Syst. Res., vol. 52, pp. 144–154, 2018, doi: 10.1016/j.cogsys.2018.06.014.
71. M. Jogin, Mohana, M. S. Madhulika, G. D. Divya, R. K. Meghana, and S. Apoorva, "Feature extraction using convolution neural networks (CNN) and deep learning," 2018 3rd IEEE Int. Conf. Recent Trends Electron. Inf. Commun. Technol. RTEICT 2018 - Proc., pp. 2319–2323, 2018, doi: 10.1109/RTEICT42901.2018.9012507.
72. S. Sharma, S. Sharma, and A. Athaiya, "Activation Functions in Neural Networks," Int. J. Eng. Appl. Sci. Technol., vol. 04, no. 12, pp. 310–316, 2020, doi: 10.33564/ijeast.2020.v04i12.054.